Optically Transparent and High Molecular Weight Polyolefin Block Copolymers toward Self-Assembled Photonic Band Gap Materials

Jongseung Yoon,[†] Robert T. Mathers,[‡,§] Geoffrey W. Coates,[‡] and Edwin L. Thomas*[,†]

Department of Materials Science and Engineering, Massachusetts Institute of Technology, Cambridge, Massachusetts 02139, and Department of Chemistry and Chemical Biology, Baker Laboratory, Cornell University, Ithaca, New York 14853

Received July 27, 2005; Revised Manuscript Received December 12, 2005

ABSTRACT: Block copolymers based on readily available olefins have been synthesized to construct self-assembled one-dimensional (1-D) photonic crystals. Using living olefin polymerization via a bis(phenoxyimine)-titanium dichloride/MAO catalyst system, optically transparent and high molecular weight polyolefin block copolymers have been prepared with a narrow molecular weight distribution. The resulting copolymers exhibited a partial 1-D photonic band gap with an excellent optical transparency. Random copolymerization of olefin monomers provided a route to tune the refractive index of each block as well as to suppress the crystallinity for optical transparency. Ternary blending of diblock copolymer with homopolymers further afforded a pathway to control the wavelength of the peak reflectivity of the polyolefin-based photonic structures.

Introduction

Photonic crystals, the optical analogue of electronic semiconductors, have gained increasing attention over the past two decades due to their unique electromagnetic properties such as inhibition of spontaneous emission,[1] photon localization,[2] and negative refraction.[3] Owing to the periodic modulation of dielectric constant (ϵ) and the Bragg scattering at domain interfaces, a photonic band gap, i.e., a finite frequency range in which the propagation of electromagnetic waves is prohibited in the material, can be formed for specific propagation directions in the crystal.[4] Numerous fabrication methods have been employed to construct photonic crystals for near-infrared and optical frequencies, ranging from "top-down" lithographic schemes such as conventional photolithography,[5,6] holographic lithography,[7,8] and coextrusion[9] to "bottom-up" approaches including self-assembly of block copolymers,[10−12] self-assembly of colloidal crystals,[13,14] and layer-by-layer assembly (by thermal evaporation, sputtering, or spin-coating).[15,16]

The well-ordered nanostructures of self-assembled block copolymers have been successfully utilized to develop one-, two-, and three-dimensional photonic crystals for visible wavelengths.[10,12,17] Block copolymers spontaneously self-assemble into different domains on the length scale of the respective blocks.[18] Various microdomain structures of block copolymers having one-, two-, and three-dimensional periodicity on nanoscopic length scales can be created by tailoring molecular parameters such as molecular weight, chain architecture, and the persistence lengths of constituent blocks or by blending with homopolymers and plasticizers. With the ability to synthesize ultrahigh molecular weight (>500 kg/mol) block copolymers so as to achieve large domain sizes that can interact with light of visible wavelength, block copolymers became promising candidate materials for constructing photonic band gap structures at optical frequencies. The versatility of block copolymer-based photonic crystals can be further increased with the possibility to add various organic/inorganic additives for creating optically active or passive multifunctional nanostructures.[19] For example, ternary blends of lamellar-forming poly(styrene-*b*-isoprene) (poly(S-*b*-I)) diblock copolymer, polystyrene, and polyisoprene were self-assembled to form a one-dimensional photonic crystal of alternating layers with a tunable photonic band gap.[10,20] Two- and three-dimensional block copolymer-based photonic crystals have also been demonstrated from the hexagonally packed cylinder and the double-gyroid cubic microstructure of poly(S-*b*-I) block copolymers, respectively.[12,17] Hierarchical structures of host diblock copolymer and hydrogen-bonded guest small molecules showed a reversible switching of the photonic band gap by altering the refractive index contrast or domain spacing under an applied thermal field.[21,22] Efforts have also been made to increase the inherently low dielectric contrast in block copolymers by selectively sequestering high index semiconductor or metal nanocrystals into a specific microdomain of block copolymer photonic crystals.[11,23]

Polyolefins have been widely used in various applications due to their versatile thermal, mechanical, and optical properties determined by their composition, chain architecture, and the tacticity.[24] Recent advances in catalyst systems for living olefin polymerization have made it possible to synthesize polyolefin-based block copolymers with precisely controlled molecular weight, molecular weight distribution, and tacticity.[25] For example, diblock copolymers of poly[syndiotactic propylene-*b*-(ethylene-*co*-propylene)] have been synthesized with a controlled molecular weight and a narrow molecular weight distribution ($M_w/M_n \sim 1.1$).[26] More recently, bis(phenoxyimine)-titanium dichloride/MAO catalysts were used for the polymerization of 1,5-hexadiene to give a random copolymer with 1,3-methylenecyclopentane (MCP) and 3-vinyltetramethylene (VTM) units.[27] The VTM units in the copolymer have been shown to undergo a cross-metathesis reaction with alkenes catalyzed by a ruthenium carbene for additional functionalization of the copolymer.[28]

The work described here is motivated by our interest in preparing polyolefin-based photonic band gap materials, which are expected to have improved thermal stability and process-

[†] Massachusetts Institute of Technology.
[‡] Cornell University.
[§] Current address: Department of Chemistry, The Penn State University New Kensington, Upper Burrell, PA 15068.
* To whom correspondence should be addressed. E-mail: elt@mit.edu.

10.1021/ma0516642 CCC: $33.50
Published on Web 02/03/2006

Scheme 1

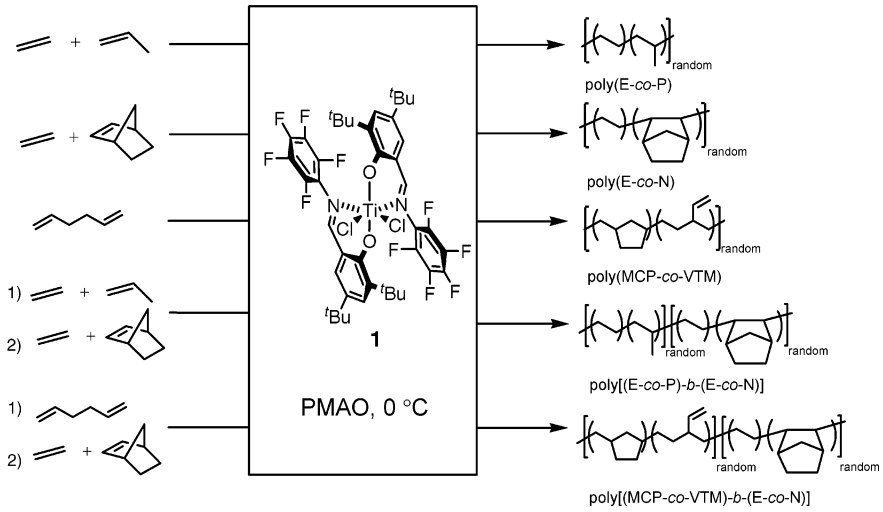

ability over more conventional diene-containing block copolymers such as poly(S-*b*-I). In this article, we present the synthesis and morphological/optical characterization of lamellar-forming polyolefin block copolymers with highly controlled molecular weight and optical transparency, which can form self-assembled 1-D photonic band gap structures.

Experimental Section

Synthesis. All air- and moisture-sensitive chemistry was carried out in a MBraun Labmaster drybox or using standard Schlenk line techniques. The solvents were dried on solvent columns containing molecular sieves, alumina, and activated copper. Propylene (Matheson, Polymer Grade) was purified by a column of molecular sieves and alumina. Ethylene (Matheson, Polymer Grade) was used as received. Polymethylaluminoxane (Akzo Nobel, PMAO-IP, 12.9 wt % Al in toluene) was dried under vacuum at 60 °C overnight. The bis(salicylaldiminato)titanium complex was prepared as previously described.[26]

a. Synthesis of Poly[(MCP-*co*-VTM)-*b*-(E-*co*-N)] Diblock Copolymer. A 6 oz. Lab-Crest glass pressure reaction vessel (Andrews Glass) was charged with PMAO (0.19 g, [Al]/[Ti] = 600), toluene (125 mL), and 1,5-hexadiene (10 mL). The reactor was equilibrated at 0 °C in an ice bath, and a catalyst solution [4 mg of **1** (Scheme 1) in 5 mL of toluene][26] was injected by syringe. After 15 min, the reactor was evacuated to remove excess 1,5-hexadiene for 5 min and backfilled with nitrogen. An aliquot (10 mL) was taken and quenched with acidic methanol. Subsequently, the norbornene (10 g in 10 mL of toluene) was injected by syringe, and ethylene was attached at 2 psi. After 29.25 h, acidic methanol (3 mL) was added by syringe to quench the polymerization. The reactor was then vented and the polymer precipitated in acidic methanol (700 mL). After stirring for several hours, the polymer was filtered, washed with methanol, and dried under vacuum (recovered 2.14 g).

b. Synthesis of Poly[(E-*co*-P)-*b*-(E-*co*-N)] Diblock Copolymer. A 6 oz. Lab-Crest glass pressure reaction vessel (Andrews Glass) was charged with PMAO (0.10 g, [Al]/[Ti] = 250) and toluene (120 mL). The reactor was weighed and placed in an ice bath. The nitrogen atmosphere in the reactor was exchanged with propylene three times. Propylene (4.0 g) was condensed into the reactor for 30 min at 10 psi. The ethylene was attached at 12 psi. The catalyst solution (10 mg of **1** (Scheme 1) in 4 mL of toluene) was injected by syringe. After 10 min, the reactor was evacuated to remove ethylene and propylene for 2 min. The reactor was backfilled with nitrogen. An aliquot (10 mL) was taken and quenched with acidic methanol. The norbornene (5 g in 10 mL of toluene) was injected by syringe. Ethylene was attached at 1.5 psi. After 21.5 h, acidic methanol (3 mL) was added to quench the polymerization. The reactor was vented and the polymer precipitated in acidic methanol (700 mL). After stirring for several hours, the polymer was filtered, washed with methanol, and dried under vacuum (recovered 2.3 g).

Characterization. The 125 MHz ^{13}C NMR data were acquired on a Varian Inova 500 spectrometer. The polymer samples were placed in a 5 mm NMR tube with 1,1,2,2-tetrachloroethane-d_2 and dissolved by heating. The data were acquired at 130 °C using an inverse gated decoupling sequence with a 5 s relaxation delay. The NMR spectra were referenced to nondeuterated solvent shifts. The copolymer microstructure was calculated according to published procedures for poly(ethylene-*co*-propylene) copolymers[26,29,30] and poly(ethylene-*co*-norbornene) copolymers.[31,32]

The molecular weights (M_n and M_w) and polydispersity indices (M_w/M_n) were measured by a Waters Alliance GPCV 2000 size exclusion chromatograph (SEC). The SEC columns (four Waters HT 6E and one Waters HT 2) were eluted at 1.0 mL/min with 1,2,4-trichlorobenzene containing 0.01 wt % di-*tert*-butylhydroxytoluene (BHT). The molecular weights (M_n and M_w) and polydispersity indices (M_w/M_n) were measured relative to a polystyrene calibration curve at 140 °C. DSC analysis was performed on a TA Instruments Q1000 equipped with an autosampler and a liquid nitrogen cooling system. Typical DSC samples (2−3 mg) were prepared in crimped aluminum pans and heated under nitrogen at a rate of 10 °C/min from −80 to +200 °C. The reported DSC data were acquired from the second heating run and processed with the TA Q Series software.

To measure the wavelength dependence of refractive index (dispersion), ellipsometry was performed using a M2000 variable angle spectroscopic ellipsometer (J.A. Woollam Co., Inc.) with 70° incidence angle. Thin films for ellipsometry (thickness ∼100 nm) of polyolefin random copolymers were prepared by spin-casting the copolymer solution on a silicon wafer. Toluene was used as a solvent for all polyolefin copolymers. Thick films for reflectivity measurement and transmission electron microscopy (TEM) (thickness ∼0.2−0.3 mm) of poly[(MCP-*co*-VTM)-*b*-(E-*co*-N)] and poly[(E-*co*-P)-*b*-(E-*co*-N)] were cast from a solution of the copolymer in toluene (∼4 wt %). To minimize defect formation during the solution casting process, a very slow evaporation condition was applied, where the evaporation of a solvent was conducted in a solvent-saturated atmosphere with a gentle flux of air, requiring 2−3 weeks for sample drying. The blends of poly[(E-*co*-P)-*b*-(E-*co*-N)] were prepared by mixing 80 wt % (60 wt %) of the host block copolymer with 10 wt % (20 wt %) of poly(E-*co*-P) (M_n = 23.2 kg/mol) and 10 wt % (20 wt %) of poly(E-*co*-N) (M_n = 23.8 kg/mol) in toluene for 20 wt % (40 wt %) blend. All samples were further dried in a vacuum at room temperature for 24 h and subsequently annealed at 120 °C for 3−10 days, producing films with a final thickness of about 0.2−0.3 mm. Ultrathin sections for TEM were obtained using a Reicht-Jung Ultracut FC4E cryomi-

Table 1. Materials Data for Polyolefin Copolymers

entry	description	E (mol %)[a]	M_n (kg/mol) (M_w/M_n)[b]	T_g (° C)[c]	n[d]	d_{001} (nm)[g]
1	poly(E-*co*-N)	62	238 (1.05)	86.5	1.52	
2	poly(E-*co*-P)	62	192 (1.09)	−58.3	1.47	
3	poly(MCP-*co*-VTM)		87 (1.12)	−19.3	1.50	
4	poly[(MCP-*co*-VTM)-*b*-(E-*co*-N)]	−/−[h]	180 (1.35)/451 (1.41)[e]	−19.3/73.1[f]		170
5	poly[(E-*co*-P)-*b*-(E-*co*-N)]	58/67	212 (1.12)/576 (1.13)[e]	−55.5/71.6[f]		91
6	poly(E-*co*-N)	67	23.8 (1.06)	69.2	1.52	
7	poly(E-*co*-P)	58	23.2 (1.11)	−56.2	1.47	

[a] Data measured by ^{13}C NMR, 130 °C, in 1,1,2,2-tetrachloroethane-d_2. [b] Data measured by GPC eluted with 1,2,4-trichlorobenzene at 140 °C relative to polystyrene standards; each value in parentheses corresponds to PDI. [c] Data measured by DSC (10 °C/min). [d] Data at 500 nm, measured by spectroscopic ellipsometry. [e] Data refer to the first polymer block/entire diblock copolymer. [f] Data refer to the first polymer block/second polymer block. [g] Domain periodicity of lamellae measured from TEM, i.e., $d_{001} = l_A + l_B$. [h] The ethylene content was not able to be obtained using ^{13}C NMR spectra since the ^{13}C NMR peaks for the poly(MCP-*co*-VTM) block were overlapped with the peaks for the poly(E-*co*-N) block. Alternatively, the glass transition temperatures (T_g) of poly[(MCP-*co*-VTM)-*b*-(E-*co*-N)] can be used to estimate the ethylene content of the copolymer since the T_g of poly(E-*co*-N) block sensitively depends on the ethylene content. Given that the glass transition temperature of poly(E-*co*-N) block of poly[(MCP-*co*-VTM)-*b*-(E-*co*-N)] (entry 4 in Table 1) is similar to that of poly(E-*co*-N) block of poly[(E-*co*-P)-*b*-(E-*co*-N)] (entry 5 in Table 1), 67% would be a reasonable estimate for the ethylene content of poly[(MCP-*co*-VTM)-*b*-(E-*co*-N)], although the effect of the other block, i.e., poly(MCP-*co*-VTM) or poly(E-*co*-P), needs to be considered for more precise estimation.

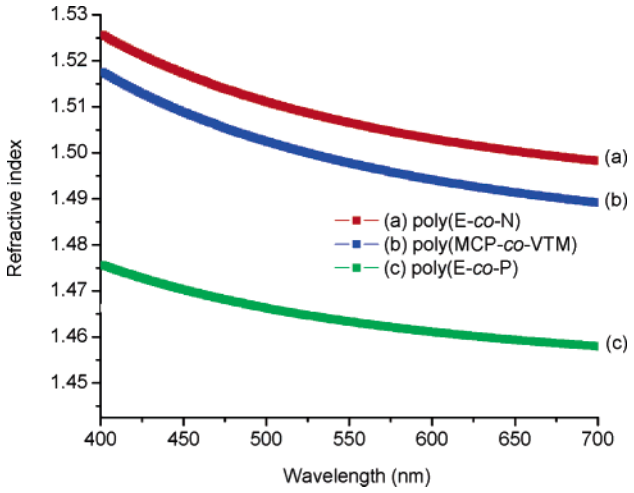

Figure 1. Refractive index as a function of wavelength for polyolefin random copolymers measured by a spectroscopic ellipsometry: (a) poly(E-*co*-N) (entry 1 in Table 1), (b) poly(MCP-*co*-VTM) (entry 3), (c) poly(E-*co*-P) (entry 2).

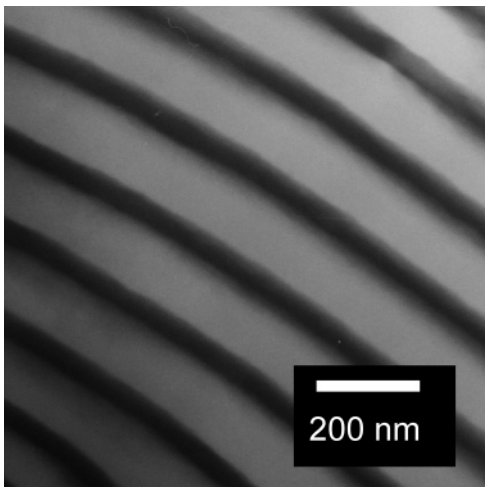

Figure 2. Bright field TEM micrograph of cryomicrotomed section of the poly[(MCP-*co*-VTM)-*b*-(E-*co*-N)] block copolymer showing a lamellar morphology (domain periodicity ~170 nm). The dark regions ($l_{MCP-co-VTM}$ = 68 nm) correspond to poly(MCP-*co*-VTM) microdomains preferentially stained with osmium tetroxide (OsO_4), and the bright regions (l_{E-co-N} = 102 nm) are poly(E-*co*-N) microdomains.

crotome. To provide mass thickness contrast between block copolymer microdomains, poly[(MCP-*co*-VTM)-*b*-(E-*co*-N)] was stained with osmium tetroxide (OsO_4) while poly[(E-*co*-P)-*b*-(E-*co*-N)] and its blends were stained with ruthenium tetroxide (RuO_4). TEM micrographs were obtained using JEOL 200CX and JEOL 2000FX microscopes operating at 200 kV. Measurement of film reflectivity spectra was conducted on a Cary 5E UV−vis−NIR spectrophotometer (Varian Inc.) equipped with a diffuse reflectance accessory. The diffuse reflectance of Halon, a compressed polyfluorocarbon powder with reflectivity above 99% over the visible wavelengths, was used as a reference spectrum. USAXS measurements of the poly[(E-*co*-P)-*b*-(E-*co*-N)] diblock copolymer and its ternary blends were performed at beamline X10A at Brookhaven National Laboratory with 8 keV radiation (wavelength $\lambda = 0.1548$ nm). A Bonse-Hart camera setup[33] was employed with single bounce Ge-111 monochromator and analyzer crystals. The slit collimated incident beam intensity was about 5×10^9 counts/s, and the beam size was 0.6×0.8 mm^2 (V-H). Data were collected by a scintillation detector (Bicron) which was swept through an arc to collect a linear data set of intensity vs angular position. All data were acquired at room temperature and used without additional corrections.

Results and Discussion

Polyolefins are often crystallizable and can exhibit a semicrystalline morphology due to the configurational regularities of the repeating units. As a result, spherulites containing chain-folded lamellae form upon crystallization and can cause a strong scattering of visible light, making polyolefins less appropriate for optical applications compared with highly transparent noncrystalline polymers such as poly(methyl methacrylate). The "random copolymer" approach employed in this study is an effective means to introduce configurational irregularities along the main chain of the copolymers, which inhibit crystallization and thus maintain optical transparency of the polyolefin block copolymers. In the design of "photonic" polyolefins, the following monomers were selected as building blocks for the synthesis of polyolefin block copolymers: ethylene (E), propylene (P), norbornene (N), and 1,5-hexadiene. Random copolymers of these monomers were synthesized with a living catalyst system to give a controlled molecular weight, a narrow molecular weight distribution, and an optical transparency, as summarized in Table 1. No melting transitions were observed in all the polyolefin random copolymers studied as determined by DSC.

A key intrinsic material property for determining a band gap of photonic crystal is the respective refractive index of each domain of the crystal. In order to tailor the dielectric contrast of polyolefin-based photonic crystals, monomers of different refractive indices were copolymerized to form a random copolymer. Polyolefin random copolymers made of the above-mentioned monomers were then evaluated to determine an effective refractive index and how the various combinations of random copolymer blocks would influence the dielectric con-

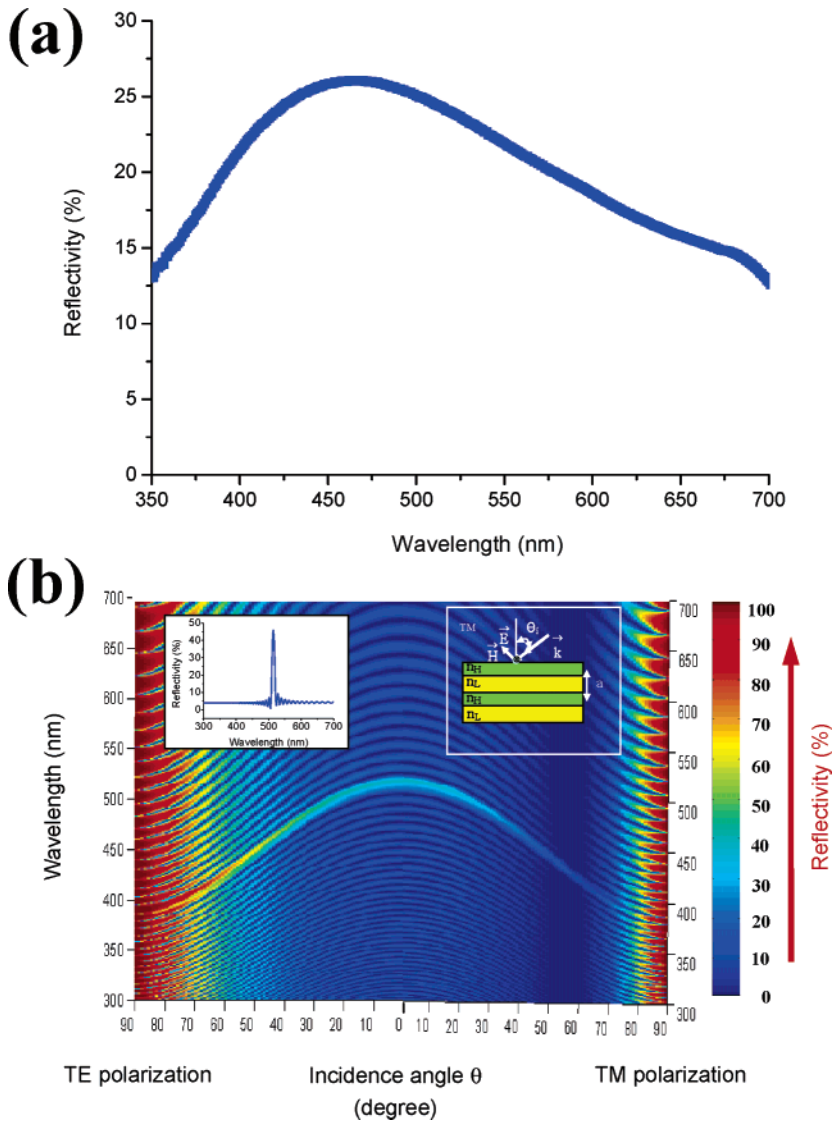

Figure 3. (a) Measured reflectivity spectrum of poly[(MCP-*co*-VTM)-*b*-(E-*co*-N)] lamellar film by a CARY spectrophotometer equipped with a diffusive reflectivity accessory. The peak reflectivity wavelength is around 470 nm. (b) Calculated reflectivity map of a multilayer stack having the same layer thickness and refractive index as poly[(MCP-*co*-VTM)-*b*-(E-*co*-N)] as a function of the incidence angle (*x*-axis), the polarization (*x*-axis), and the wavelength (*y*-axis) of the incident light, assuming the thickness of high (E-*co*-N)/low (MCP-*co*-VTM) index layer is 102 nm/68 nm, the refractive index of high/low index layer is 1.52/1.50, and a total number of 100 layers. The inset (upper left) shows the reflectivity spectrum at normal incidence (incidence angle = 0°) as a function of wavelength, in which the peak reflectivity wavelength is 515 nm. The inset (upper right) shows a schematic of TM polarized light (magnetic field is perpendicular to the plane of incidence) incident on the multilayer stack with an incidence angle θ (E: electric field vector; H: magnetic field vector; k: wave vector; n_H: refractive index of high index layer; n_L: refractive index of low index layer; a: domain periodicity).

trast. Figure 1 shows the wavelength dependence of the refractive index for various polyolefin random copolymers, as measured by spectroscopic ellipsometry over the visible wavelength range. Clearly the refractive index ($= \epsilon^{1/2}$, where ϵ is a dielectric constant of medium) can be readily tuned by simply varying the combination of different monomers. As shown in Figure 1, in ethylene-containing random copolymers, poly(E-*co*-N) ($n \sim 1.52$ at 500 nm) exhibited higher refractive index than poly(E-*co*-P) ($n \sim 1.47$ at 500 nm) at the same ethylene content (62%) due to the lower refractive index of polypropylene ($n \sim 1.47-1.49$)[34] than polynorbornene ($n \sim 1.52-1.54$).[35]

On the basis of the evaluation of refractive index and thermal properties, two sets of polyolefin diblock copolymers, poly-[MCP-*co*-VTM)-*b*-(E-*co*-N)] and poly[(E-*co*-P)-*b*-(E-*co*-N)], were synthesized by a sequential monomer addition. These block copolymer systems were soluble in toluene at room temperature and showed no detectable crystallinity by DSC. Table 1 summarizes the detailed information on the synthesized block copolymers. TEM was performed on thermally annealed films of the copolymers after cryomicrotomy and staining. Figure 2 shows a bright field TEM micrograph of a poly[(MCP-*co*-VTM)-*b*-(E-*co*-N)]. A lamellar morphology exhibiting a periodicity of about 170 nm is clearly evident with alternating layers of poly(MCP-*co*-VTM) and poly(E-*co*-N). The dark regions correspond to poly(MCP-*co*-VTM) domains, in which VTM units containing the alkene group were preferentially stained with osmium tetroxide (OsO_4) while the bright regions correspond to the poly(E-*co*-N) domains.

A self-assembled block polymer having a lamellar morphology can form a multilayer stack of one-dimensionally periodic index of refraction or a 1-D photonic crystal. To examine the optical properties of the self-assembled 1-D photonic film, a reflectivity spectrum was obtained by a CARY spectrophotometer equipped with a diffusive reflectivity accessory. As shown in Figure 3a, the spectrum of poly[MCP-*co*-VTM)-*b*-(E-*co*-N)] copolymer film exhibited a reflectivity band resulting from the

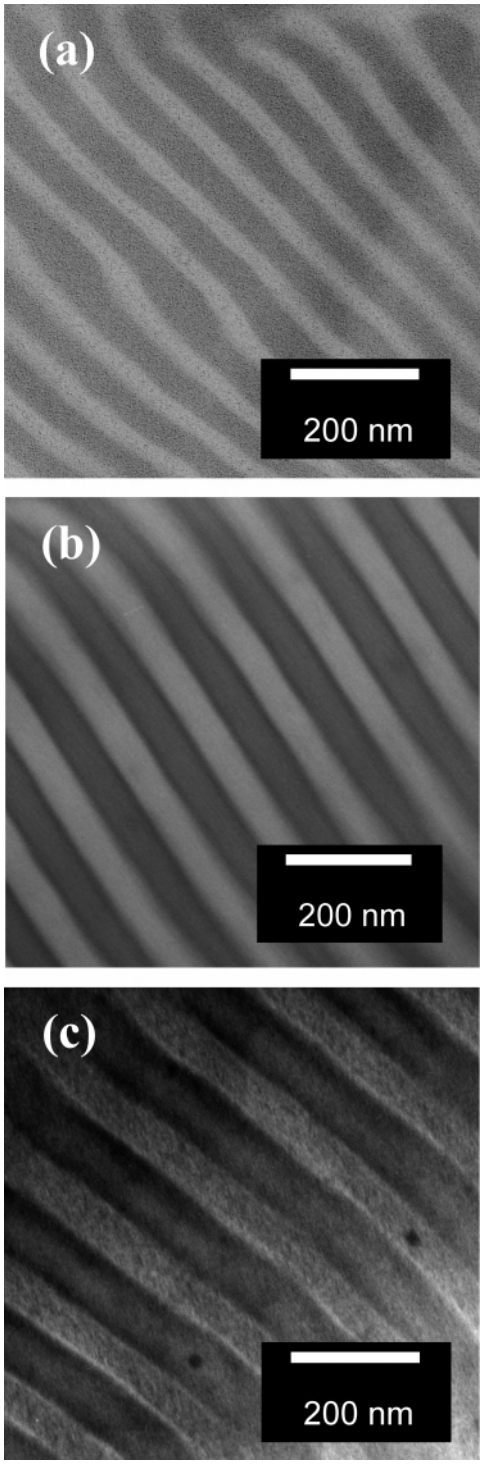

Figure 4. Bright field TEM micrographs of cryomicrotomed sections of the poly[(E-*co*-P)-*b*-(E-*co*-N)] and its ternary blends: (a) host diblock copolymer of poly[(E-*co*-P)-*b*-(E-*co*-N)], (b) ternary blend containing 20 wt % (10/10) homopolymers, (c) ternary blend containing 40 wt % (20/20) homopolymers. The domain periodicity is 91 nm (l_{E-co-N} = 56 nm, l_{E-co-P} = 35 nm) for the host diblock and is increased to 127 nm (l_{E-co-N} = 79 nm, l_{E-co-P} = 48 nm) and 152 nm (l_{E-co-N} = 88 nm, l_{E-co-P} = 64 nm) for the ternary blends containing 20 and 40 wt % homopolymers. The dark regions correspond to poly(E-*co*-N) microdomains preferentially stained with ruthenium tetroxide (RuO_4), and the bright regions correspond to poly(E-*co*-P) microdomains. Small particle-like entities in the micrographs come from ruthenium tetroxide (staining agent) aggregations.

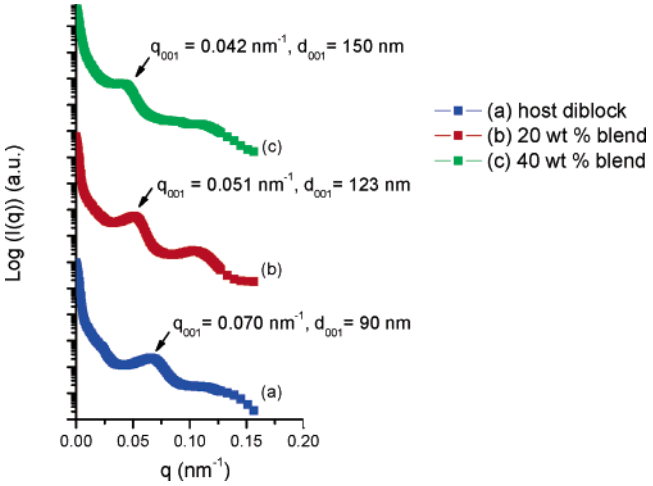

Figure 5. Smeared USAXS 1-D line source data obtained from the polyolefin block copolymer films of (a) the poly[(E-*co*-P)-*b*-(E-*co*-N)] and ternary blends of the diblock containing (b) 20 wt % and (c) 40 wt % homopolymers. The (001) peaks for all three samples correspond well to the lamellar periods measured from TEM micrographs.

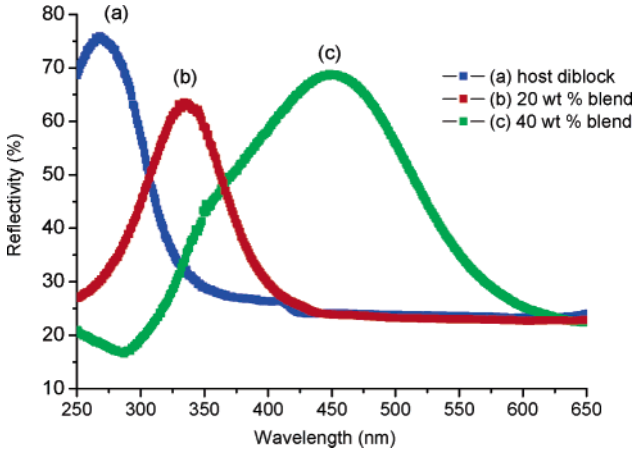

Figure 6. Measured reflectivity spectra of (a) the poly[(E-*co*-P)-*b*-(E-*co*-N)] and ternary blends of the diblock containing (b) 20 and (c) 40 wt % homopolymers by a CARY spectrophotometer equipped with a diffusive reflectivity accessory. The peak reflectivity wavelengths are (a) 268 nm (host diblock), (b) 335 nm (20 wt % blend), and (c) 448 nm (40 wt % blend).

effect of partial 1-D photonic band gap, where the peak reflectivity was centered around 470 nm. A convenient way to understand the obtained reflectivity spectrum is to model the 1-D block copolymer photonic structure with a stack of finite number of alternating layers, for which optical properties can be readily calculated by a transfer matrix method (TMM).[21,36] Although the computational result with this simple model does not capture all the microstructural details of the block copolymer photonic structure such as the variation of domain size, domain orientation, and randomly located defects, it can provide a useful reference to correlate the obtained reflectivity spectrum with morphological properties of the block copolymer photonic structure. Figure 3b shows a calculated "reflectivity map" of the corresponding model 1-D multilayer (100 layers) stack of poly[MCP-*co*-VTM)-*b*-(E-*co*-N)], in which the measured thicknesses (102 nm/68 nm) and refractive indices (1.52/1.50) of the lamellar domains have been used for the calculation and the magnitude of the reflectivity was visualized using different colors as a function of the incidence angle (*x*-axis), the polarization (*x*-axis), and the wavelength (*y*-axis) of the incident light. The inset (upper right) in Figure 3b shows a schematic of TM polarized light (magnetic field is perpendicular to the plane of incidence) incident on the multilayer stack with an angle θ. The region of high reflectivity in Figure 3b, or a partial 1-D

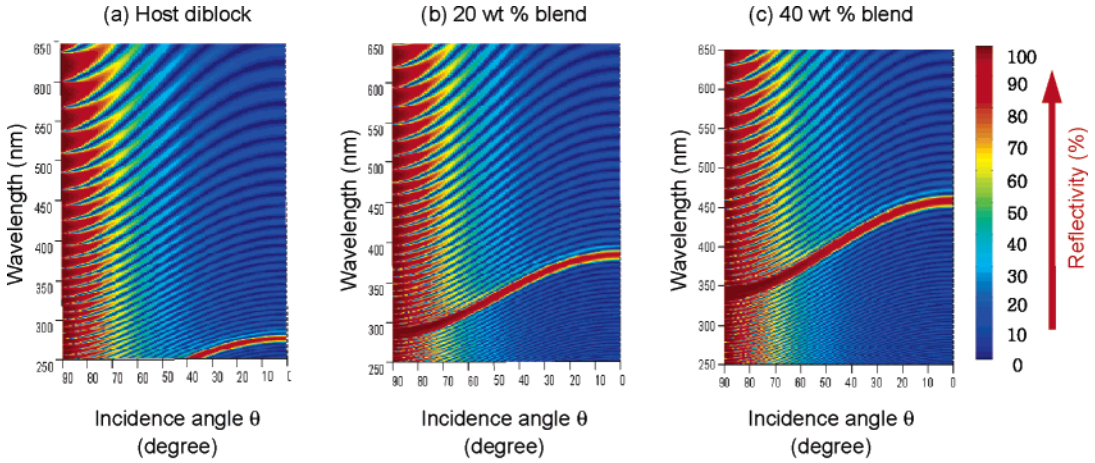

Figure 7. Calculated reflectivity maps (for TE polarization of incident light) of multilayer stacks having the same layer thickness and refractive index as (a) poly[(E-*co*-P)-*b*-(E-*co*-N)], (b) 20 wt %, and (c) 40 wt % ternary blend as a function of the incidence angle (*x*-axis) and the wavelength (*y*-axis) of incident light, assuming that the thickness of high (E-*co*-N)/low (E-*co*-P) index layer is (a) 56 nm/35 nm, (b) 79 nm/48 nm, and (c) 88 nm/64 nm as obtained from TEM, the refractive index of high/low index layer is 1.52/1.47 as obtained from ellipsometry, and a total number of 100 layers.

photonic band gap, results from a constructive interference of incident light at the set of 1-D periodic interfaces between the high and low refractive domains. The band gap of the 1-D photonic crystal blue-shifts to a shorter wavelength as the incidence angle is increased from zero (normal incidence) to grazing angle. A reflectivity spectrum at a specific incidence angle and polarization can be extracted from a reflectivity map. For example, the inset (upper left) in Figure 3b shows a cross section of the reflectivity map at normal incidence of light (i.e., incidence angle $\theta = 0°$). The calculated peak reflectivity wavelength at normal incidence is around 515 nm while the observed peak reflectivity wavelength is about 470 nm. It is also shown that the width (FWHM) of the measured reflectivity spectrum is much broader than that of the calculated reflectivity spectrum. These comparisons essentially suggest that the lamellar domains of the current block copolymer system are not perfectly oriented along the normal incidence direction but have a distribution of different microdomain orientations. If we assume that the misorientation of lamellae is the dominant factor for the observed reflectivity, the average lamellar orientation (deviation from the normal incidence) can be estimated as 38°, at which the peak reflectivity wavelength is 470 nm from the TMM calculation. Indeed, the self-assembled block copolymer microstructures tend to consist of multiple grains of various domain orientations. The measured reflectivity spectrum in Figure 3a should be therefore interpreted as the superposed spectral response of many different grains having the distribution of domain thickness, domain orientation, and randomly located defects. To do more precise and quantitative modeling of the reflectivity spectrum, we would have to take into account all the above-mentioned microstructural details of the block copolymer photonic structure as well as the optical loss from absorption and scattering.

To further engineer the photonic properties of this poly[(MCP-*co*-VTM)-*b*-(E-*co*-N)] block copolymer, a postpolymerization reaction can be conducted to incorporate a fluorine-containing (low-index) moiety into the poly(MCP-*co*-VTM) block and thus to increase the dielectric contrast. The effect of fluorine-containing group on the microphase separation (increase of Flory−Huggins interaction parameter, χ) and optical properties (increase of Δn by about a factor of 5×) of the block copolymer is currently under investigation.

Another polyolefin diblock copolymer, poly[(E-*co*-P)-*b*-(E-*co*-N)], was synthesized using the same living catalyst system. On the basis of the refractive index and DSC measurements, poly[(E-*co*-P)-*b*-(E-*co*-N)] is expected to have a larger dielectric contrast ($\Delta n \sim 0.05$) and be more thermally stable (containing no alkene group in the main chain) than poly[(MCP-*co*-VTM)-*b*-(E-*co*-N)]. In this block copolymer system, we further blended lower molecular weight homopolymers of each block, i.e., 10 wt % (20 wt %) of poly(E-*co*-P) (M_n: 23.2 kg/mol) and 10 wt % (20 wt %) of poly(E-*co*-N) (M_n: 23.8 kg/mol), with 80 wt % (60 wt %) of the host diblock copolymer, poly[(E-*co*-P)-*b*-(E-*co*-N)] (M_n: 212 kg/mol/364 kg/mol), to swell the lamellar microdomains and to therefore tune the photonic band gap of the block copolymer photonic crystal to a longer wavelength range. Figure 4a−c shows bright field TEM micrographs of the host poly[(E-*co*-P)-*b*-(E-*co*-N)] diblock copolymer and ternary blends of the diblock (80 wt %, 60 wt %) and each homopolymer (10 wt %, 20 wt %), in which the lamellar morphology, composed of dark (E-*co*-N) domains (stained with ruthenium tetroxide (RuO_4)) and bright (E-*co*-P) domains, was clearly identified. As shown in Figure 4a−c, the domain periodicity was increased from 91 to 127 nm (20 wt % blend) and to 152 nm (40 wt % blend) as a result of swelling of microdomains with added homopolymers. The corresponding smeared 1-D ultrasmall-angle X-ray scattering (USAXS) data of the samples are presented in Figure 5, where the shift in the first-order peak of scattering vector (q_{001}) to a lower value supports the increase of domain periodicity (d_{001}) in the ternary blends observed in TEM. The domain periodicities obtained from USAXS are good agreement with those observed from TEM. To further confirm the samples have lamellar morphologies, tilting experiments in TEM, which can provide a clear difference between lamellar and cylindrical morphologies, have been conducted, and no oblique or end-on views of cylindrical domains have been observed from extensive investigation of many microtomed cross-sectioned samples. In Figure 6, we show the reflectivity spectra of the host diblock and ternary blend samples measured by a CARY spectrophotometer equipped with a diffusive reflectivity accessory. The peak reflectivity wavelength for the host block copolymer sample occurs at 268 nm and is red-shifted to 335 nm (20 wt %) and to 448 nm (40 wt %) for the ternary blends as the optical thickness (domain refractive index × domain thickness) of the blended samples is increased by swelling with added homopolymers. For further analysis of the measured reflectivity spectra, TMM calculations have been conducted on the basis of measured domain thicknesses (from

TEM) and refractive indices (from ellipsometry). Figure 7 shows the reflectivity map for corresponding model 1-D multilayer (100 layer) stacks of the host diblock and ternary blends for TE polarization of incident light, in which the peak reflectivity wavelengths at normal incidence are shown to be 273 nm (host diblock), 382 nm (20 wt % blend), and 456 nm (40 wt % blend). The measured reflectivity spectra of the blend samples (Figure 6) are in reasonable agreement with the calculated reflectivity map (Figure 7) in terms of the peak reflectivity wavelengths. As mentioned earlier, the lower values (blue-shift) of the measured peak reflectivity wavelength compared with calculated values at normal incidence of light result from the deviation of the average lamellar orientation from normal incidence. The broadness of the measured reflectivity spectra in Figure 6 can be understood by considering the polygrained nature of the cast films containing lamellae of various domain orientations, domain thicknesses, and randomly located defects. The assignment of lamellar morphologies is also supported by the obtained reflectivity spectra. Calculation of reflectivity for 2-D photonic crystal of hexagonally packed cylinders having an equal periodicity to 1-D lamellar structure predicts a peak reflectivity at much lower wavelength.[17]

In conclusion, we have shown that self-assembled lamellar block copolymers based on readily available olefins can be employed to create 1-D photonic structures in the visible wavelength range. With a suitable choice of a catalyst system for living olefin polymerization, polyolefin block copolymers having a large molecular weight have been prepared with a narrow molecular weight distribution. The resulting copolymers, poly[(MCP-*co*-VTM)-*b*-(E-*co*-N)] and poly[(E-*co*-P)-*b*-(E-*co*-N)], exhibited a partial 1-D photonic band gap with an excellent optical transparency. Random copolymerization of olefin monomers provided a means to tune the refractive index contrast and to suppress the crystallinity of the polyolefin block copolymers. Ternary blending of the diblock copolymers with homopolymers further afforded a pathway to control the accessible peak reflectivity wavelength of the polyolefin-based photonic structures. Further studies for improvements over the current system including the effect of selective fluorination on the morphology and optical properties of polyolefin block copolymers are underway.

Acknowledgment. The authors thank the National Science Foundation for financial support under Grant 0103297 (NSF-NIRT). This research made use of experimental facilities at the Center for Materials Science and Engineering at MIT and the Cornell Center for Materials Research Shared Experimental Facilities supported by NSF. G. W. Coates gratefully acknowledges support from the Packard and Sloan Foundation. J.Yoon and E. L. Thomas also acknowledge the Brookhaven National Laboratory (beamline X10A) for performing the USAXS measurements. Use of the National Synchrotron Light Source, Brookhaven National Laboratory, was supported by the U.S. Department of Energy, Office of Science, Office of Basic Energy Sciences, under Contract DE-AC02-98CH10886.

References and Notes

(1) Ogawa, S. P.; Imada, M.; Yoshimoto, S.; Okano, M.; Noda, S. *Science* **2004**, *305*, 227−229.
(2) Ozaki, R.; Matsuhisa, Y.; Ozaki, M.; Yoshino, K. *Appl. Phys. Lett.* **2004**, *84*, 1844−1846.
(3) Luo, C.; Johnson, S. G.; Joannopoulos, J. D.; Pendry, J. B. *Phys. Rev. B* **2002**, *65*, 2011041−2011044.
(4) Joannopoulos, J. D.; Meade, R. D.; Winn, J. N. *Photonic Crystals: Molding the Flow of Light*; Princeton University Press: Princeton, 1995.
(5) Foresi, J. S.; Villeneuve, P. R.; Ferrera, J.; Thoen, E. R.; Steinmeyer, G.; Fan, S.; Joannopoulos, J. D.; Kimerling, L. C.; Smith, H. I.; Ippen, E. P. *Nature (London)* **1997**, *390*, 143−145.
(6) Noda, S.; Tomoda, K.; Yamamoto, N.; Chutinan, A. *Science* **2000**, *289*, 604−606.
(7) Campbell, M.; Sharp, D. N.; Harrison, M. T.; Denning, R. G.; Turberfield, A. J. *Nature (London)* **2000**, *404*, 53−56.
(8) Ullal, C. K.; Maldovan, M.; Thomas, E. L.; Chen, G.; Han, Y. J.; Yang, S. *Appl. Phys. Lett.* **2004**, *84*, 5434−5436.
(9) Weber, M. F.; Stover, C. A.; Gilbert, L. R.; Nevitt, T. J.; Ouderkirk, A. J. *Science* **2000**, *287*, 2451−2456.
(10) Urbas, A.; Fink, Y.; Thomas, E. L. *Macromolecules* **1999**, *32*, 4748−4750.
(11) Bockstaller, M.; Kolb, R.; Thomas, E. L. *Adv. Mater.* **2001**, *13*, 1783−1786.
(12) Urbas, A. M.; Maldovan, M.; DeRege, P.; Thomas, E. L. *Adv. Mater.* **2002**, *14*, 1850−1853.
(13) Tarhan, II; Watson, G. H. *Phys. Rev. Lett.* **1996**, *76*, 315−318.
(14) Wijnhoven, J.; Vos, W. L. *Science* **1998**, *281*, 802−804.
(15) Fink, Y.; Winn, J. N.; Fan, S. H.; Chen, C. P.; Michel, J.; Joannopoulos, J. D.; Thomas, E. L. *Science* **1998**, *282*, 1679−1682.
(16) Chen, K. M.; Sparks, A. W.; Luan, H. C.; Lim, D. R.; Wada, K.; Kimerling, L. C. *Appl. Phys. Lett.* **1999**, *75*, 3805−3807.
(17) Deng, T.; Chen, C. T.; Honeker, C.; Thomas, E. L. *Polymer* **2003**, *44*, 6549−6553.
(18) Park, C.; Yoon, J.; Thomas, E. L. *Polymer* **2003**, *44*, 6725−6760.
(19) Edrington, A. C.; Urbas, A. M.; DeRege, P.; Chen, C. X.; Swager, T. M.; Hadjichristidis, N.; Xenidou, M.; Fetters, L. J.; Joannopoulos, J. D.; Fink, Y.; Thomas, E. L. *Adv. Mater.* **2001**, *13*, 421−425.
(20) Urbas, A.; Sharp, R.; Fink, Y.; Thomas, E. L.; Xenidou, M.; Fetters, L. J. *Adv. Mater.* **2000**, *12*, 812−814.
(21) Osuji, C.; Chao, C. Y.; Bita, I.; Ober, C. K.; Thomas, E. L. *Adv. Funct. Mater.* **2002**, *12*, 753−758.
(22) Valkama, S.; Kosonen, H.; Ruokolainen, J.; Haatainen, T.; Torkkeli, M.; Serimaa, R.; Ten Brinke, G.; Ikkala, O. *Nat. Mater.* **2004**, *3*, 872−876.
(23) Fink, Y.; Urbas, A. M.; Bawendi, M. G.; Joannopoulos, J. D.; Thomas, E. L. *J. Lightwave Technol.* **1999**, *17*, 1963−1969.
(24) Galli, P.; Vecellio, G. *J. Polym. Sci., Part A: Polym. Chem.* **2004**, *42*, 396−415.
(25) Coates, G. W.; Hustad, P. D.; Reinartz, S. *Angew. Chem., Int. Ed.* **2002**, *41*, 2236−2257.
(26) Tian, J.; Hustad, P. D.; Coates, G. W. *J. Am. Chem. Soc.* **2001**, *123*, 5134−5135.
(27) Hustad, P. D.; Coates, G. W. *J. Am. Chem. Soc.* **2002**, *124*, 11578−11579.
(28) Mathers, R. T.; Coates, G. W. *Chem. Commun.* **2004**, 422−423.
(29) Wang, W. J.; Zhu, S. P. *Macromolecules* **2000**, *33*, 1157−1162.
(30) Hustad, P. D.; Tian, J.; Coates, G. W. *J. Am. Chem. Soc.* **2002**, *124*, 3614−3621.
(31) Tritto, I.; Marestin, C.; Boggioni, L.; Zetta, L.; Provasoli, A.; Ferro, D. R. *Macromolecules* **2000**, *33*, 8931−8944.
(32) Yoshida, Y.; Mohri, J.; Ishii, S.; Mitani, M.; Saito, J.; Matsui, S.; Makio, H.; Nakano, T.; Tanaka, H.; Onda, M.; Yamamoto, Y.; Mizuno, A.; Fujita, T. *J. Am. Chem. Soc.* **2004**, *126*, 12023−12032.
(33) Bonse, U.; Hart, M. *Z. Phys.* **1966**, *189*, 151.
(34) Brandrup, J.; Immergut, E. H.; Grulke, E. A. *Polymer Handbook*, 4th ed.; Wiley-Interscience: New York, 1999.
(35) Haselwander, T. F. A.; Heitz, W.; Krugel, S. A.; Wendorff, J. H. *Macromol. Chem. Phys.* **1996**, *197*, 3435−3453.
(36) Born, M.; Wolf, E. *Principle of Optics*, 7th ed.; Cambridge University Press: Cambridge, 1999.

MA0516642